doi:10.3788/gzxb20174606.0622001

用于校准能见度仪的标准散射体定标系统中光学系统的设计

张健[1],张国玉[1,2,3],徐达[1],孙高飞[1,2,3],苏拾[1,2,3],张建良[4]

(1 长春理工大学,长春 130022)

(2 光电测控与光电信息传输技术教育部重点实验室,长春,130022)

(3 吉林省光电测控仪器工程技术研究中心,长春 130022)

(4 空军航空大学,长春 130022)

摘 要:为了实现校准能见度仪中标准散射体的快速准确定标,建立了用于校准能见度仪的标准散射体的定标系统.研究了定标系统中全景成像折反光学系统的设计方法.根据抛物面反射镜的光学特性推导出抛物面面型的计算方法.根据定标系统对光学系统的要求,完成全景成像色度计光学系统的设计.对全景成像折反光学系统进行建模仿真并设计实验验证光学系统的设计与仿真结果的正确性.实验结果表明:全景成像折反光学系统的空间检测俯仰角范围为 0°~90°,方位角范围为 0°~360°,且最小角分辨率为 1°,与仿真结果基本一致,满足用于校准能见度仪的标准散射体定标系统中光学系统的设计要求.

关键词:仪器光学设计;前向散射式能见度仪;全景成像光学系统;校准;散射测量

中图分类号:TH765.8+3 **文献标识码**:A **文章编号**:1004-4213(2017)06-0622001-9

Optical System Design of the Standard Scattering Plate Calibration System Used in Calibration Visibility Meter

ZHANG Jian[1], ZHANG Guo-yu[1,2,3], XU Da[1], SUN Gao-fei[1,2,3], SU Shi[1,2,3], ZHANG Jian-liang[4]

(1 *Changchun University of Science and Technology, Changchun* 130022, *China*)

(2 *Key Laboratory of Optical Control and Optical Information Transmission Technology, Department of Education, Changchun* 130022, *China*)

(3 *Optical Measurement and Control Instrumentation, Jilin Province Engineering Research Center, Changchun* 130022 *China*)

(4 *Aviation University of Air Force, Changchun* 130022, *China*)

Abstract: In order to realize the rapid and high precision calibration of standard scattering plate, the standard scattering plate calibration system used in calibration visibility meter was established. The design method of panoramic imaging colorimeter optical system of the calibration system was researched. Based on the optical properties of parabolic reflector, the calculation method of paraboloid surface was deduced. Then, according to the requirement of the calibration system optical system, the design of optical system of panoramic imaging colorimeter optical system was completed. Finally, the panoramic imaging colorimeter optical system was modeling analyzed, and an experiment was designed to verifies the

Foundation item: The National Public Welfare Industry Science and Technology Projects in China (Nos. GYHY200706003, GYHY201006043)

First author: ZHANG Jian (1989-), male, Ph. D degree candidate, mainly focuses on meteorological instruments, photoelectric instrument and testing technology. Email:zhangjian_nr@126.com

Supervisor: ZHANG Guo-yu (1962-), male, professor, Ph. D. degree, mainly focuses on space science and technology, photoelectric instrument and testing technology. Email:zh_guoyu@163.com

Received: Dec. 15, 2016; **Accepted**: Mar. 7, 2017

correctness of the design and simulation results. The experiment shows that the spatial measuring range is in the range of incident angle from 0° to 90° and azimuth angle from 0° to 360°; and the angular resolution is 1° which satisfy the design requirements of the optical system of the standard scattering plate calibration system used in a calibration visibility meter.

Key words: Optical design of instruments; Forward scattering visibility meter; Panoramic imaging optical system; Calibration; Scattering measurements

OCIS Codes: 220.0220; 120.4570; 290.2558; 290.5820

0 Introduction

Atmospheric horizontal visibility, which is an important physical quantity that represents the atmosphere pollution degree of the subsurface, has a great influence on the aviation, navigation, transportation and military actions[1]. The main instruments for visibility measurement are transmission type visibility meter, forward scattering type visibility meter, backward scattering type visibility meter, Digital Photography Visiometer System (DPVS) and laser radar. On account of the convenience of installation, usage and maintenance for the forward scattering type visibility meter, it has been widely used. But, the forward scattering type visibility meter within a certain range of visibility is still with larger error of measurement, so there were some researches on improving the precision of forward scattering type visibility meter and studying its calibration method at home and abroad.

Huang Xin, et al proposed to combine of lenses and step-index fiber to limit the receiver's field angle, suppressed the most outside stray light effect on measurement results of visibility[2]. Zhao Jing, et al proposed to construct high precision forward scatter visibility meter launch system with high power LED light source to improve the measuring accuracy of forward scatter visibility meter[3]. Li Hao, et al deduced the detection equation of forward scatter visibility meter, analyzed the error source of forward scatter visibility meter and their uncertainty[4]. Wang Qing-mei[5], Cheng Yin[6] and Wang Mian[7], et al proposed some method to use scattering plates to calibrate forward scattering type visibility meter. Zhu Le-Qun, et al proposed the condition and method of lab calibration of forward scattering type visibility meter, summed up and sorted out the methods of optical device calibration at work site, calibrated plate calibration, and manual calibration[8]. At present, in the foreign, the calibration method of standard scattering plate used in a calibration visibility meter is mainly the calibration method for the standard scattering plate in the Vaisala FD12P calibration method which was put forward by Royal Netherlands Meteorological Institute (KNMI)[9]. Currently, domestic researches for improving accuracy of forward scatter visibility meter mainly focus on improving the related part of forward scatter visibility meter via analyzing the error of the forward scattering type visibility meter or studying the calibration method of the forward scattering type visibility meter. Meanwhile, there are some issues on the current international standard calibration methods of scattering calibration, such as its calibration time is long, calibration chain is complex, error transfer links of calibration are too many, calibration efficiency is low, and this method to calibrate forward scatter visibility meter only can implement outdoors and so on. So far, the study of calibration method for the standard scattering plate used in calibrating the forward scatter visibility meter is still few.

The standard scattering plate of the forward scattering type visibility meter utilizes its scattering coefficient to simulate the corresponding visibility conditions. With the rapid development of the measurement of bi-directional scattering distribution function, it realizes calibration by measuring the scattering coefficient of the standard scattering plate[10-19].

In this paper, we bring the measurement of bi-directional scattering distribution function in the calibration of standard scattering plate, design a calibration system of standard scattering plate by measuring its scattering coefficient. The composition and working principle of the calibration system were presentation. The design process and modeling analysis of panoramic imaging refractive and reflective optical system were described. And an experiment was designed to verifies the correctness of the design and the simulation results. The panoramic imaging refractive and reflective optical system provides excellent foundation for the subsequent correction of lateral misalignment of the imaging points in accordance with the measurement principle of the standard scattering calibration system for calibrating

visibility meter, the design of the electrical system and the construction of the calibration method.

1 The composition and working principle of calibration system

1.1 The calibrating principle of using a standard scattering plate to calibrate a forward scattering type visibility meter

The definition of meteorology for visibility is that the maximum distance which the eyes with standard vision can distinguish the black body targets contour from the background of sky on the horizontal direction[20]. The results of visibility measured by human eyes are always different, due to the difference of awareness, resolving power and light source characteristics. In order to define the visibility objectively, World Meteorological Organization (WMO) proposed to use atmospheric transparency to evaluate the visibility in 1957. Visibility expressed as Meteorological Optical Range (MOR), and the definition of MOR is the distance which luminous flux of parallel light exited from the incandescent light bulb under the condition that color temperature of 2 700 k is attenuated to the 5% of the initial luminous flux[21].

According to the Koschmieder's law[22], when black body targets are on the background of sky, the contrast between the apparent brightness of the targets and the background can be expressed as Eq. (1).

$$R_m=\frac{1}{\sigma}\ln\frac{1}{\varepsilon} \tag{1}$$

In the Eq. (1), R_m is weather range of visibility, $\varepsilon$is contrast threshold of human vision, σ is atmospheric extinction coefficient.

Atmospheric extinction coefficient σ is the sum of scattering coefficient K_s and absorption coefficient K_a. The absorption effect of atmospheric aerosol is much less than the scattering effect of atmospheric aerosol. According to provisions of the WMO, the visibility V can be expressed as Eq. (2).

$$V=\frac{-\ln\varepsilon}{K_s} \tag{2}$$

Based on the Mie scattering theory[23], when the range of scattering angle θ of atmospheric aerosol is between 20°and 50°, the relationship among scattered light intensity $I(\theta)$, scattering coefficient K_s, and incident intensity I_0 can be expressed as Eq. (3)[24].

$$I(\theta)=K_sI_0 \tag{3}$$

According to the Eqs. (2) and (3), forward scattering type visibility meter can measure the visibility V indirectly by measuring the scattering coefficient K_s, and the standard scattering plate can simulate the different visibility V by simulating different scattering coefficients K_s to calibrate the forward scattering type visibility meter.

1.2 The composition and working principle of calibration system

According to the Eqs. (2) and (3), when $\varepsilon=0.05$, the relationship among scattered light intensity $I(\theta)$, visibility V, and incident intensity I_0 can be expressed as Eq. (4).

$$V=\frac{2.996I_0}{I(\theta)}=\frac{2.996}{I(\theta)/I_0} \tag{4}$$

Based on the Eq. (4), only if a standard scattering plate calibration system used in calibration visibility meter can measure the scattered light intensity $I(\theta)$ and the incident intensity I_0 of scattering angle θ, can the visibility V which is simulated by the standard scattering plate be measured.

The the standard scattering plate calibration system used in calibration visibility meter is consist of high uniformity stable lighting system, low reflectivity imaging sphere system, and panoramic imaging colorimeter[25]. The system composition is shown in Fig. 1.

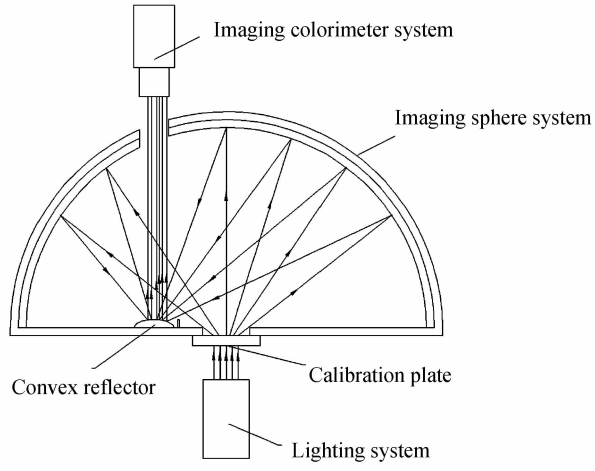

Fig. 1 System composition

The light beams emitted from the high uniformity stable lighting systemm scatter on the inner surface of the low reflectivity imaging sphere system after they shine uniformly and penetrate the standard scattering, and form the optical field distribution in the inner surface of the low reflectivity imaging sphere system after scattered by the standard scattering. The field of view of the panoramic imaging colorimeter optical system is enlarged by the parabolic reflector, thus realizing the collection of the energy distribution of the inner wall of the entire low reflectivity imaging sphere system. The scattering coefficient of the standard scattering in each scattering angle is obtained through the software. The visibility simulated by the standard scatting plate can be calibrated. The working principle of the calibration system is shown in Fig. 2.

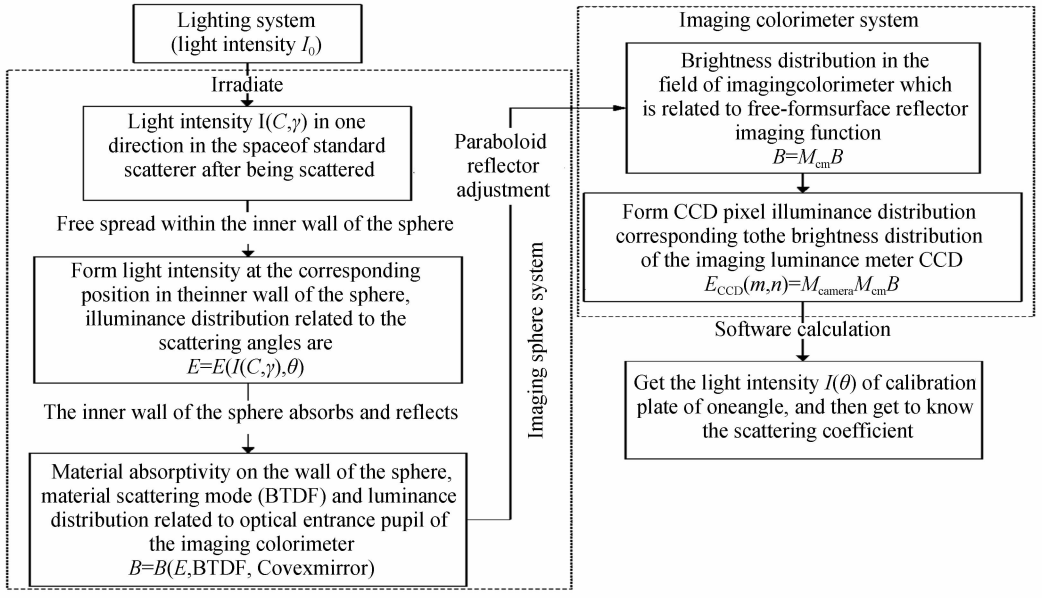

Fig. 2 Working principle of the system

2 Design of the panoramic imaging refractive and reflective optical system

The optical sysytem of the calibration system is a panoramic imaging refractive and reflective optical system which is consisted of the paraboloid reflector in the low reflectivity imaging sphere system and the panoramic imaging colorimeter optical system. The optical model of the system is shown in Fig. 3. In the Fig. 3, β_1 and β_2 represent the incident angle of incident ray 1 and incident ray 2 .

2.1 Design of the parabolic surface

As parabolic surface is the rotational symmetric curved surface, there is only a need to deduct in the two-dimensional space[26]. According to the working principle of the optical system, assume that the equation of the parabolic reflecting surface is $z = z(r)$; the incident light will converge at point O , its

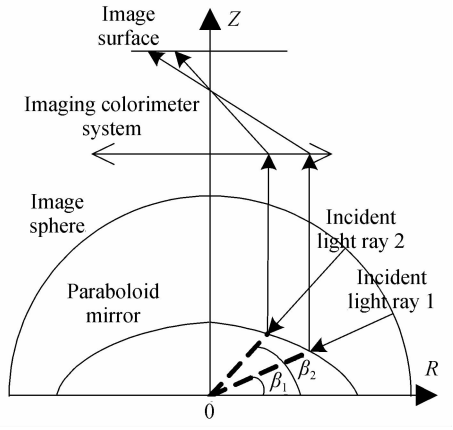

Fig. 3 Optical model of the system

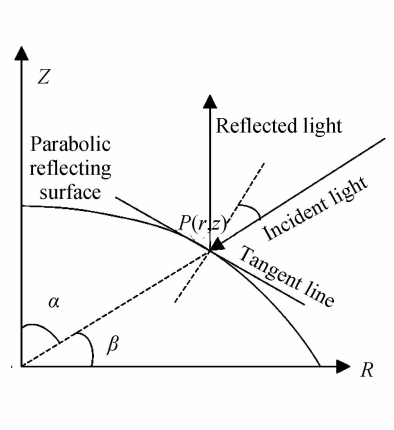

Fig. 4 Optical path diagram of the parabolic reflector

included angle with the Z-axis is α, the incident angle is β, the reflected light parallels to the Z-axis, and the coordinate of the point of incidence P is (r, z). The optical path of the parabolic reflector is shown in Fig. 4.

The expression of the parabolic reflecting surface can be expressed as Eq. (5).

$$z=\frac{H^2-r^2}{2H} \tag{5}$$

In Eq. (5) H is the integration constant, which reflects the surface type of the parabolic reflector. It is shown in Fig. 5.

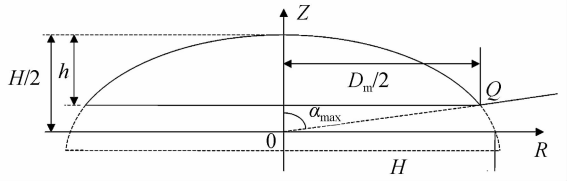

Fig. 5 Diagrammatic figure of the parabolic reflector

Assume that $r=\rho\sin\alpha$ and $z=\rho\cos\alpha$, then the poplar equation of the parabolic reflector is expressed as Eq. (6).

$$\rho=\frac{H}{1+\cos\alpha} \tag{6}$$

Assume that the caliber of the reflector is D_M, the angle of field of view of the system in the height direction is α_{max}, point Q (r_Q, z_Q) at the bottom of the reflector, so that we can obtain the Eq. (7).

$$H^2-D_M\cot(\alpha_{max})H-\frac{D_M^2}{4}=0 \tag{7}$$

It can be figured out from Fig. 5 that the thickness of the reflector is expressed as Eq. (8)

$$h=\frac{H}{2}-z_Q=\frac{D_M}{4}\left[\frac{\cos(\alpha_{max})+1}{\sin(\alpha_{max})}\right]-\frac{D_M}{2}\cot(\alpha_{max})=\frac{D_M[1-\cos(\alpha_{max})]}{4\sin(\alpha_{max})} \tag{8}$$

$D_M=25$ mm and $\alpha_{max}=90°$ are selected according to the system indicators, thus the thickness of the parabolic surface is $h=6.25$ mm. The equation of the parabolic surface is expressed as Eq. (9).

$$r^2=-25z+\frac{625}{4} \tag{9}$$

2.2 Design of panoramic imaging colorimeter optical system

According to the requirements of the calibration system index, the optical system angular resolution of the panoramic imaging colorimeter is 1°. Thereinto, the sensor dimension of the panoramic imaging colorimeter optical system is 1 024 pixel× 1 024 pixel; each pixel dimension is 5.5 μm× 5.5 μm; image plane dimension is 5.6 mm× 5.6 mm; object height is 25 mm; object distance is 451.09 mm.

According to Eq. (9), the incident angle β, and object-image relationship of the panoramic imaging colorimeter that the minimum resolution of the incident ray for the principal plane is 0.109 mm; and the minimum resolution of the incident ray for the image surface is 0.024 mm. The relation between r and β is shown in Fig. 6.

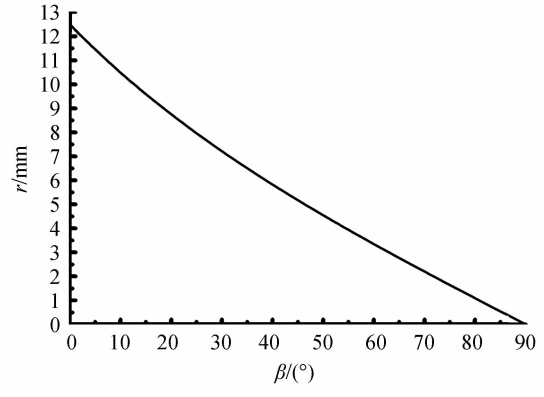

Fig. 6 Relation diagram between r and β

According to the analysis above, it is known that this system is a small field of view optical system with medium aperture; the light from various incident angles from the inner wall of the imaging sphere should be distinguished in the image plane, so that the light information of all fields of view can be analyzed; as a result, the distortion of the optical system should be as small as possible. Therefore, the optical system mainly corrects the spherical aberration, coma, curvature of the field and the distortion.

The double-gluing lens, with the positive lens of N-LASF41 from Schott and the negative lens of

LASF35 from Schott, is selected as the initial structure of the system. The spherical aberration and the coma of the selected initial structure are corrected to some extent, while the curvature of the field and the distortion receive no good correction; in addition, it can be seen from the MTF curve that the imaging quality of the optical system can not meet the requirements, thus further optimization of the optical system is needed.

It can get to know from the primary aberration Saydy composite numbers that $\sum S_{\mathrm{I}} = 0$ and $\sum S_{\mathrm{II}} = 0$ after the system corrects the spherical aberration and the coma; and it can be known from the Saydy composite numbers that the astigmatism $\sum S_{\mathrm{III}} = 0$. Add a negative field lens behind the system to correct the curvature of the field and the distortion, and the off-axis light of that piece of mirror has relatively great angle of incidence i_z, so that it can produce negative $\sum S_{\mathrm{IV}}$ to balance the curvature of the field of the system. The effect of the negative field lens on the spherical aberration, coma and the focal power is little, and the focal power is determined by the requirements of correcting the curvature of the field[27]; meanwhile, the overall bending of the lens is used to correct the distortion. The design parameters of the final optical system are shown in Table 1.

Table 1 Design indexes of the optical system

Focal length	Height of the object surface	Object distance	Image plane resolution	Angular resolution
84 mm	25 mm	451.09 mm	0.024 mm	1°

The optimized system curvature of the field as well as the distortion curves, spot diagram, MTF curve and the wave aberration are shown in Fig. 7.

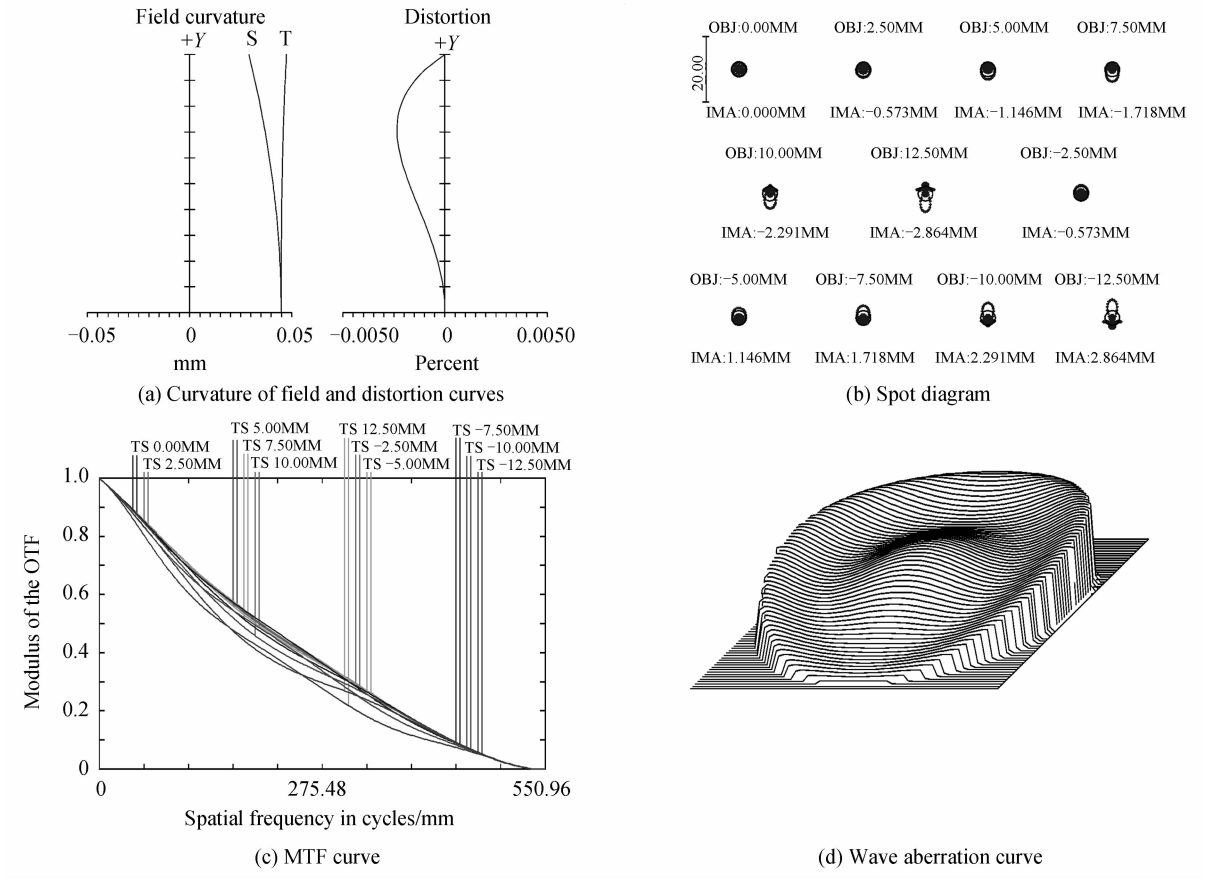

Fig. 7 Imaging quality evaluation map of the optimized system

The system curvature of the field is smaller than 0.05, and the relative distortion is smaller than 0.005%; the geometric radiuses of the spot diagrams of all optical fields of view are all smaller than 5.6 μm; the MTF curves of all fields of view approach the diffraction limit; the wavefront aberration curve of the optical system is the worst in the greatest field of view, and the root-mean-square value of the wave aberration is not greater than 0.094λ, which is smaller than 1/10λ. It can be judged from the above

aberration analysis that the designed optical system possesses excellent imaging quality and can satisfy the operating requirements.

3 Simulation and experimental verification

According to Fig. 1, the panoramic imaging colorimeter related to the low reflectivity imaging sphere system is in off-axis condition, and, the off-axis deviation of the system itself can be corrected through later period algorithm; as a result, simulation verification on the panoramic imaging refractive and reflective optical system can be conducted under non-off-axis condition.

3.1 Simulation of the spatial measuring range

Select two vertical diameters in the low reflectivity imaging sphere system, and set a point light source at an interval of 30° in the range of incident angle β from 0° to 90°, so as to verify the spatial measuring range of the panoramic imaging refractive and reflective optical system. The simulation results are shown in Fig. 8. It can be seen from the figure that all the point light sources in the range of incident angle β from 0° to 90° and azimuth angle from 0° to 360° can be formed in the image plane of the panoramic imaging colorimeter, thus the panoramic imaging refractive and reflective optical system can realize the measurement of the entire spatial intensity distribution characteristics of the imaging sphere.

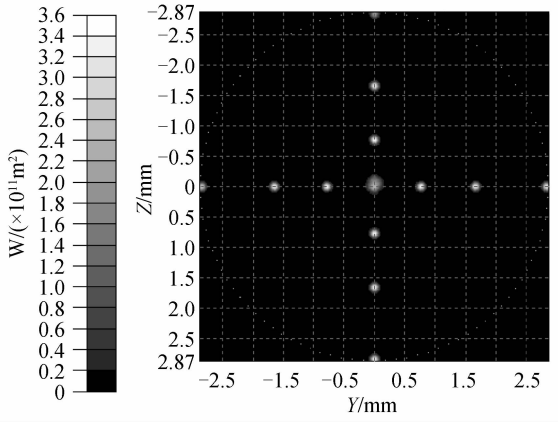

Fig. 8 Image plane illuminance simulation diagram of the spatial measuring range

3.2 Simulation of the minimum angular resolution

It can be figured out from Fig. 6 that greater angle of incidence of the light source β is associated with higher requirements of the system resolution. Therefore, select a diameter of the imaging sphere, and set a point light source from the angle of incidence of 80° to 90° at an interval of 1°, with an aim to verify whether the system satisfies the requirements of the minimum angular resolution. The simulation results are shown in Fig. 9.

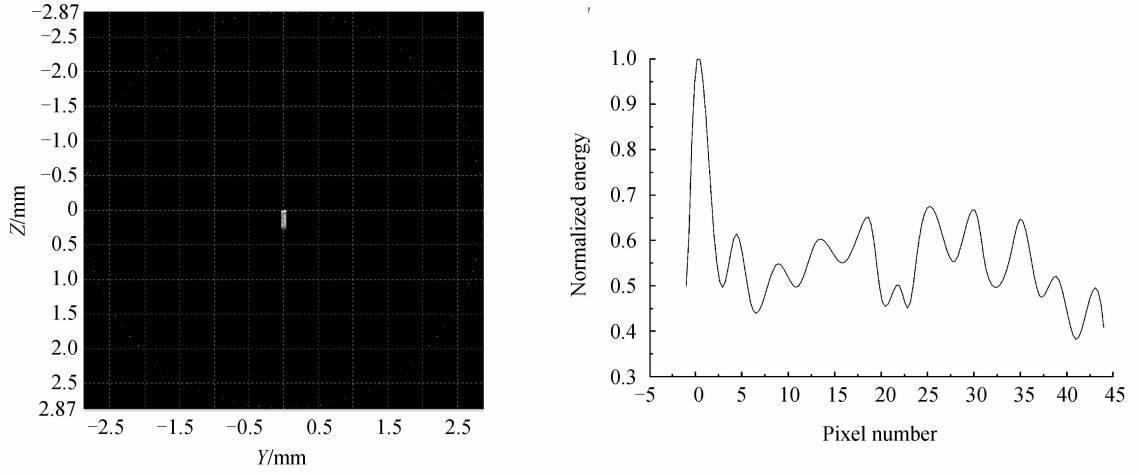

Fig. 9 Image plane illuminance simulation diagram of the minimum angular resolution

It can be seen from the figure that within the range of 80° to 90°, the system satisfies the requirement of the minimum angular resolution being 1°, which means that within the range of 0° to 90°, the system satisfies the requirement of the minimum angular resolution being 1°.

3.3 Experimental verification

In order to verify the simulation results of the panoramic imaging refractive and reflective optical system, we use two rotating platforms, a laser and a parabolic reflector to set a test platform under non-off-axis condition. It is shown in Fig. 10.

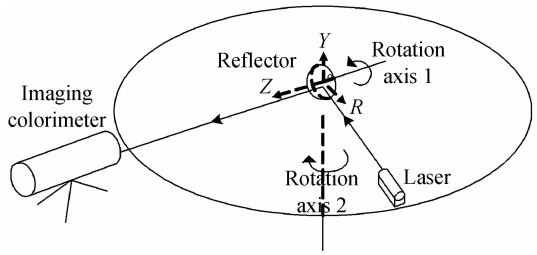

Fig. 10 Schematic diagram of the test platform

In Fig. 10, rotation axis 1 drives the reflector to rotate around axis Z regarding the reflector center as the center of rotation; rotation axis 2 drives the laser to rotate around axis Y regarding the reflector center as the center of rotation; and the light emitted by the laser enters into the panoramic imaging colorimeter after reflection of the reflector. It can realize the simulation of laser to the illuminating conditions of any point of the reflector, and simulate the inwall imaging conditions within the entire low reflectivity imaging sphere system collected by the panoramic imaging colorimeter via the rotation of the laser and the reflector. We regulate the rotation axis 1 and rotation axis 2 every 20° in order to validate the simulation results of the spatial detection range of the panoramic imaging refractive and reflective optical system. We can rotate the rotation axis 2 to make the incident angle α of the laser vary 1° every time within the range of 80°～90° (Due to the dimensional limitation of the experimental facilities themselves, the incident angle range during the practical experimental process is 80°～87°). And then, we can simulate the minimum angular resolution of the panoramic imaging refractive and reflective optical system. The experimental results are shown in Fig. 11.

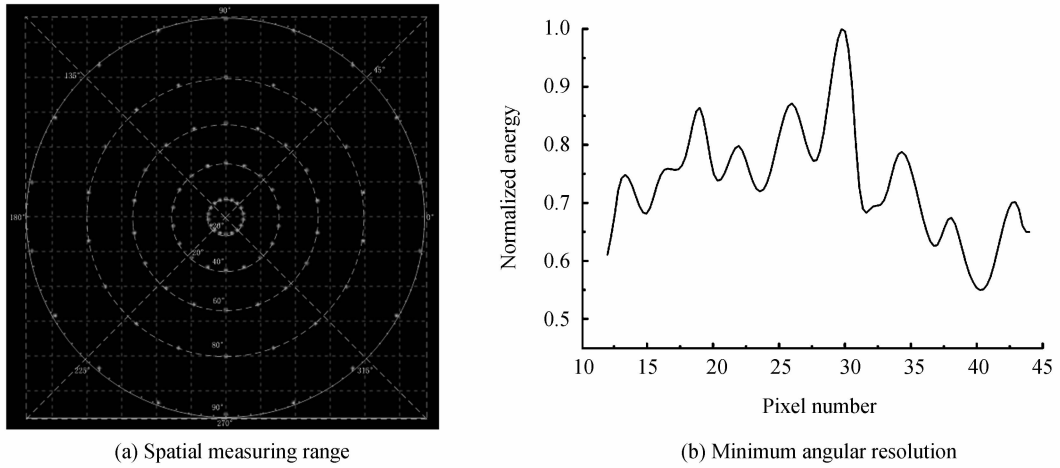

(a) Spatial measuring range (b) Minimum angular resolution

Fig. 11 Experimental results pictures

In Fig. 11, we can conclude that the spatial measuring range is incident angle β from 0°to 90° and azimuth angle from 0°to 360°; and the angular resolution is 1° were agreement with the simulation results of software which meet the measurement requirement of the intensity distribution character within the entire low reflectivity imaging sphere system.

4 Conclusion

Aiming at the long calibration time, complex calibration chain and many calibration error transfer links of standard scattering plate, a calibration of standard scattering plate by measuring the scattering coefficient of the standard scattering plate was established. The composition and working principle of the calibration system, the design process and modeling analysis of panoramic imaging refractive and reflective optical system were described. And an experiment was designed to verifies the correctness of the design and the simulation results. The experiment proves: the spatial measuring range is incident angle from 0°to 90° and azimuth angle from 0° to 360°; and the angular resolution is 1° which satisfy the design requirements of the optical system of the standard scattering plate calibration system used in a calibration visibility meter.

References

[1] HU Lin. Software design of a visibility meter[D]. University of Electronic Science and Technology of China, 2012.
[2] HUANG Xin. Study of improving the uncertainty of the scattering visibility mete[D]. Nanjing: Nanjing University of Information Science & Technology, 2013.
[3] ZHAO Jing, XIAO Shao-rong. The design of high precision visibility meter launch system[J]. *Science Technology and Engineering*, 2013, **13**(33): 9950-9953.
[4] LI Hao, SUN Xue-jin. Theoretical analysis on measurement error of forward scattering visibility meter[J]. *Infrared and Leaser Engineering*, 2009, **38**(6): 1094-1098.
[5] WANG Qing-mei, XIE Bang-li, MEI Pin-chen, *et al*. Discussing the theory and calibration of the forward scatter metter [J]. *Meteorological, Hydrological and Marine Instruments*, 2001(4):10-16.
[6] CHEN Yin. A calibration method of forward scattering type visibility meter: China, 103278478 A[P]. 2013-09-04.
[7] WANG Mian, LIU Wen-qing, LU Yi-Huai, *et al*. Calibration and correction methods for the transform coefficients of the atmospheric visibility system by aerosol forward-scattering theory[J]. *Optical technique*, 2008, **34**(3): 334-337.
[8] ZHU Le-kun, LI Lin. Calibration techniques for forward scattering visibility meters[J]. *Meteorological Science and Technology*, 2013, **41**(6): 1003-1007.
[9] BLOEMINK H I. KNMI visibility standard for calibration of scatterometers[C]. 4th ICEAWS International Conference on Experiences with Automatic Weather Stations, Lisboa, Portugal. 2006.
[10] BARTELL F O, DERENIAK E L, WOLFE W L. The theory and measurement of bidirectional reflectance distribution function /BRDF/ and bidirectional transmittance distribution function /BTDF/[C]. SPIE, 1980, **257**: 154-160.
[11] STUHLINGER T W, DERENIAK E L, BARTELL F O. Bidirectional reflectance distribution function of gold-plated sandpaper[J]. *Applied Optics*, 1981, **20**(15): 2648-2655.
[12] DAVIS L, KEPROS J G. Improved facility For BRDF/BTDF optical scatter measurements[C]. SPIE, 1986, **675**: 24-32.
[13] CADY F M, STOVER J C, BJORK D R, *et al*. Design review of a multiwavelength, three-dimensional scatterometer [C]. San Dieg - DL Tentative. International Society for Optics and Photonics, 1990.
[14] DROLEN B L. Bidirectional reflectance and surface specularity results for a variety of spacecraft thermal control materials[C]. 26th Thermophysics Conference Honolulu, HI, USA. 1991.
[15] MIETTINEN J, HARKONEN A K, PIIRONEN T H. Optical scattering measurement instrument for the design of machine vision illumination[C]. SPIE, 1992, **1614**: 45-56.
[16] TSUCHIDA S, SATO I, OKADA S. Measurement of land surface BRDF with spatial instability for vicarious calibration[C]. Sensors, Systems, and Next-Generation Satellites III. Sensors, Systems, and Next-Generation Satellites III, 1999.
[17] KLAASSEN T O, SMORENBURG K. Reflectance measurements on submillimeter absorbing coatings for HIFI[C]. SPIE, 2000, **4013**: 129-139.
[18] DANA K J. BRDF/BTF measurement device[C]. ICCV 2001, Eighth IEEE International Conference on Computer Vision. 2001,2:460-466 .
[19] WADMAN S, BAUMER S. Appearance characterization by a scatterometer employing a hemispherical screen[C]. SPIE, 2003, **5189**: 163-173.
[20] LI Chun-liang. Hundred questions of visibility measurement technique[M]. China Meteorological Press, 2009.
[21] WMO G. WMO Guide to meteorological instruments and methods of observation. WMO-No. 8[M]. Secretariat of the World Meteorological Organization, 1983, I9-1.
[22] ZHANG Cheng-chang. A course of atmospheric aerosol[M]. China Meteorological Press, 1995.
[23] ZHOU Xiu-ji. Advanced atmospheric physics[M]. China Meteorological Press, 1991.
[24] YU Rong-bin. A research on testing theory and technology improving forward direction light scattering of small angle [D]. South China Normal University, 2002.
[25] RYKOWSKI R, CHITTIM K, WADMAN S. Imaging sphere enables rapid source, intensity mapping[J]. *Photonics Spectra*, 2005, **39**(9): 64-69.
[26] DUAN Ying-li. Catadioptric panorama imaging system design on the basis of aspheric surface[D]. Xi′an: Xidian University, 2012.
[27] XU Da, ZHANG Guo-yu, SUN Gao-fei. Optical system design for static ultraviolet earth simulator [J]. *Optoelectronic Engineering*, 2014(8): 85-89.